Electronic Supporting Information

Synthesis of reduced graphene oxide–based catalytic complexes for benzylamine–*o*-phenylenediamine oxidative coupling

Dheeraj, [a] Lata Rana [a,*] and Kuldeep Mahiya,[b]

[a]*Department of Chemistry, S. V. National Institute of Technology Surat, icchanath, Surat 395007; E-mail: latarana@chem.svnit.ac.in*

[b]*Department of Chemistry, FGM Govt. College Adampur Hisar 125052, Haryana, India.*

Experimental section

Physical characterization

Elemental analysis of the prepared complexes was carried out employing an Elementar vario-EL III elemental analyzer. Infrared (IR) spectra were obtained with a Shimadzu FT-IR spectrometer. 1H-NMR spectra were noted on a Bruker 600 MHz spectrometer employing NMR solvent as DMSO-d_6. The weight loss and thermal stability of the complexes were recorded employing a TA Instruments thermal analyzer (Model SDTQ 600). Powder X-ray diffraction studies were recorded on PANalytical AERIS diffractometer over a 2θ range of 5° to 50°, with a scanning rate of 0.2° per minute. FE-SEM and HR-TEM were noted on Carl Zeiss Gemini microscope and JEOL-2100F instrument, respectively. X-ray photoelectron spectroscopy (XPS) of the prepared compounds were determined on a PHI 5000 VersaProbe II system. Surface area measurements were performed using a Quantachrome NOVA 2200E instrument based on the Brunauer–Emmett–Teller (BET) method.

Crystal structure determination

A metallic light orange block-shaped crystal of complex **1** and a clear light orange block-shaped crystal of complex **2** was mounted on the goniometer. Data for both were collected from a shock-cooled single crystal at 100.00 K on a Bruker APEX-II CCD diffractometer with Mo/K_α radiation (λ = 0.71073 Å). All data were integrated with SAINT V8.40B and a multi-scan and numerical absorption correction using SADABS 2016/2 was applied.[1,2] The structure was solved by dual methods with SHELXT and refined by full-matrix least-squares methods against F2 using SHELXL.[3,4] All calculations were conducted within the OLEX[2] crystallographic suite.[5] All non-hydrogen atoms were refined with anisotropic displacement parameters. All hydrogen atoms were refined with isotropic displacement parameters. All

hydrogen atoms on carbon were fixed geometrically with U_{iso} values of 1.2 and 1.5 times the U_{iso} values of phenylene and methyl carbons and the hydrogen on oxygen of hydroxyl groups and water molecules were located from difference fourier map and refined with fixed distances (0.85 Å) with U_{iso} values of 1.5 times the U_{iso} values of their carrier atoms. Crystallographic data for the structures reported in this paper have been deposited with the Cambridge Crystallographic Data Centre.[6] CCDC 2502676 and 2502677 contain the supplementary crystallographic data for this paper. These data can be obtained free of charge from The Cambridge Crystallographic Data Centre *via* www.ccdc.cam.ac.uk/structures. Table S1 shows the crystal data and structural refinement parameters for both compounds. Tables S2 provide a summary of the selected bond lengths and bond angles.

Table S1. Crystal data and structure refinement for complexes **1** and **2.**

	Complex **1**	Complex **2**
CCDC number	**2502676**	**2502677**
Empirical formula	$C_{16}H_{18}MoN_2O_9$	$C_{17}H_{22}MoN_2O_{11}$
Formula weight	478.26	526.30
Temperature [K]	100.00	100.00
Crystal system	monoclinic	monoclinic
Space group (number)	$P2_1/n$ (14)	$P2_1/c$ (14)
a [Å]	12.3289(5)	12.2318(9)
b [Å]	11.9065(4)	6.9036(5)
c [Å]	12.6831(4)	23.6607(18)
α [°]	90	90
β [°]	105.6990(10)	92.445(2)
γ [°]	90	90
Volume [Å^3]	1792.35(11)	1996.2(3)
Z	4	4
ρ_{calc} [gcm^{-3}]	1.772	1.751
μ [mm^{-1}]	0.787	0.723
F(000)	968	1072
Crystal size [mm^3]	0.288×0.215×0.134	0.139×0.052×0.023
Crystal colour	metallic light orange	clear light orange
Crystal shape	block	block
Radiation	MoK_α (λ=0.71073 Å)	MoK_α (λ=0.71073 Å)
2θ range [°]	4.85 to 60.96 (0.70 Å)	3.33 to 49.99 (0.84 Å)
Index ranges	$-17 \le h \le 15$, $-15 \le k \le 15$, $-17 \le l \le 18$	$-14 \le h \le 14$, $-8 \le k \le 8$, $-28 \le l \le 28$
Reflections collected	35349	37445
Independent reflections	4784, R_{int} = 0.0344, R_{sigma} = 0.0258	3522, R_{int} = 0.0962, R_{sigma} = 0.0548
Completeness to θ = 24.996°	99.4 %	100.0 %
Data / Restraints / Parameters	4784/5/274	3522/8/304
Absorption correction	0.8311/0.9305 (numerical)	0.6780/0.7454 (multi-scan)
Goodness-of-fit on F^2	1.088	1.041
Final R indexes [$I \ge 2\sigma(I)$]	R_1 = 0.0238, wR_2 = 0.0657	R_1 = 0.0419, wR_2 = 0.0946
Final R indexes [all data]	R_1 = 0.0251, wR_2 = 0.0667	R_1 = 0.0603, wR_2 = 0.1011
Largest peak/hole [eÅ^{-3}]	0.45/−0.62	0.59/−0.90

Tables S2. Selected bond lengths and bond angles for Complexes **1** and **2**.

Bond lengths (Å)		Complex 1		Complex 2		Bond angles (°)	Complex 1		Complex 2	
Atom	**Atom**	**Obs.**	**Calc.**	**Obs.**	**Calc.**	**Atoms**	**Obs.**	**Calc.**	**Obs.**	**Calc.**
Mo1	O1	2.0143(9)	2.012	2.010(3)	1.980	O1 Mo1 O5	80.31(4)	80.78	79.23(11)	78.45
Mo1	O2	1.9302(9)	1.983	1.903(3)	1.897	O1 Mo1 N1	71.60(4)	71.34	71.38(11)	70.56
Mo1	O3	1.7042(9)	1.767	1.710(3)	1.680	O2 Mo1 O1	150.27(4)	146.98	149.46(11)	145.90
Mo1	O4	1.7092(10)	1.690	1.691(3)	1.678	O2 Mo1 O5	82.51(4)	81.34	81.51(11)	80.56
Mo1	O5	2.3219(10)	2.305	2.287(3)	2.256	O2 Mo1 N1	80.67(4)	79.90	81.64(12)	80.23
Mo1	N1	2.2425(11)	2.223	2.235(3)	1.234	O3 Mo1 O1	97.53(4)	98.96	96.03(12)	95.23
O1	C9	1.3179(16)	1.876	1.325(4)	1.309	O3 Mo1 O2	103.84(4)	105.34	105.01(12)	105.45
O2	C16	1.3533(15)	1.986	1.352(5)	1.336	O3 Mo1 O4	105.54(5)	106.23	105.30(14)	104.67
N1	N2	1.3998(15)	1.329	1.396(4)	1.378	O3 Mo1 O5	81.76(4)	82.45	83.28(12)	84.90
N1	C10	1.2946(16)	1.234	1.292(5)	1.278	O3 Mo1 N1	155.91(4)	153.98	159.16(13)	157.23
N2	C9	1.3091(16)	1.256	1.312(5)	1.309	O4 Mo1 O1	96.13(4)	95.34	95.86(13)	93.56
O6	C5	1.3557(16)	1.346	1.355(5)	1.324	O4 Mo1 O2	97.76(4)	97.93	99.54(13)	99.08
O7	C1	1.4296(17)	1.409	1.426(5)	1.408	O4 Mo1 O5	172.32(4)	176.90	170.63(12)	170.45
O7	C6	1.3686(16)	1357	1.386(5)	1.367	O4 Mo1 N1	97.12(4)	96.23	92.75(12)	91.45
O8	C2	1.4334(16)	1.423	1.439(5)	1.432	N1 Mo1 O5	75.32(4)	74.23	78.14(10)	77.45

Computational investigations

Theoretical investigations were performed using the Gaussian 09 software package.[7] All geometry optimizations for the ligands and their corresponding complexes were carried out using the B3LYP level of theory.[8] The 6-31G(d,p) basis set was applied for ligand atoms, while the LANL2DZ basis set was employed for the transition metal centres. Frequency analyses were conducted on the optimized structures to confirm the absence of imaginary frequencies (Table S5), thereby validating the stability of the minima. The computed vibrational frequencies exhibited good agreement with experimental data. In the solution phase, the magnetic shielding tensors of ^{1}H and ^{13}C nuclei were calculated using the Gauge-Independent Atomic Orbital (GIAO) method (Table S6 and S7). To simulate solvation effects, the Integral Equation Formalism Polarizable Continuum Model (IEFPCM) was employed, with DMSO-d_6 as the implicit solvent.[9-11] The resulting chemical shift values provided reliable insight into the electronic environments of the ligands and metal complexes.

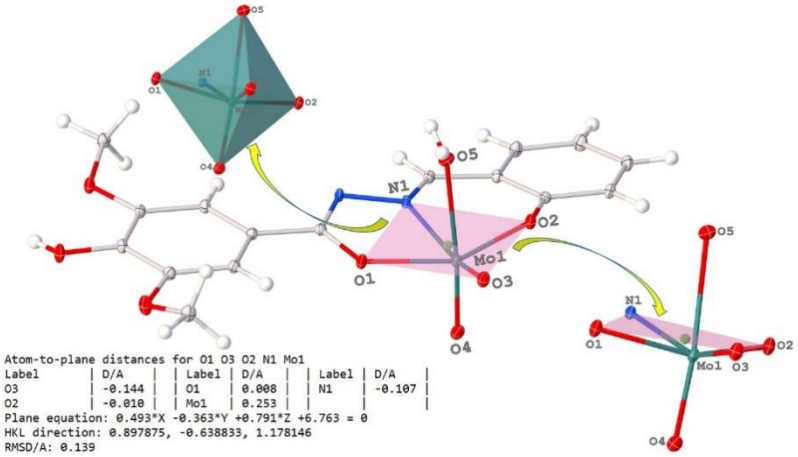

Figure S1. ORTEP diagram of complex **1** depicting octahedral geometry around Mo(VI) center and equatorial plan (the deviation of each atoms and root mean deviation from the plan is shown in the figure).

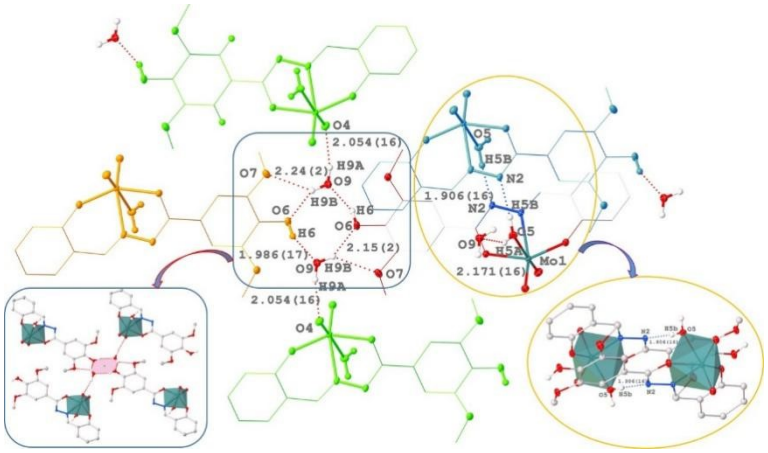

Figure S2. Diagram showing different kind of hydrogen bonding present in complex **1**.

Table S3. Hydrogen Bonds for complex **1**

D	H	A	d(D-H)/Å	d(H-A)/Å	d(D-A)/Å	D-H-A/°
O5	H5A	O9[1]	0.802(14)	2.171(16)	2.8860(14)	148.6(18)
O5	H5B	N2[2]	0.837(15)	1.906(16)	2.7422(15)	176(2)
O6	H6	O9	0.817(16)	1.986(17)	2.7667(14)	160(2)
O9	H9A	O4[3]	0.824(15)	2.054(16)	2.8659(14)	168(2)
O9	H9B	O6[4]	0.818(17)	2.15(2)	2.8682(14)	147(2)
O9	H9B	O7[4]	0.818(17)	2.24(2)	2.8904(15)	137(2)

[1]-1/2+x,3/2-y,-1/2+z; [2]1-x,1-y,1-z; [3]+x,1+y,+z; [4]2-x,2-y,1-z

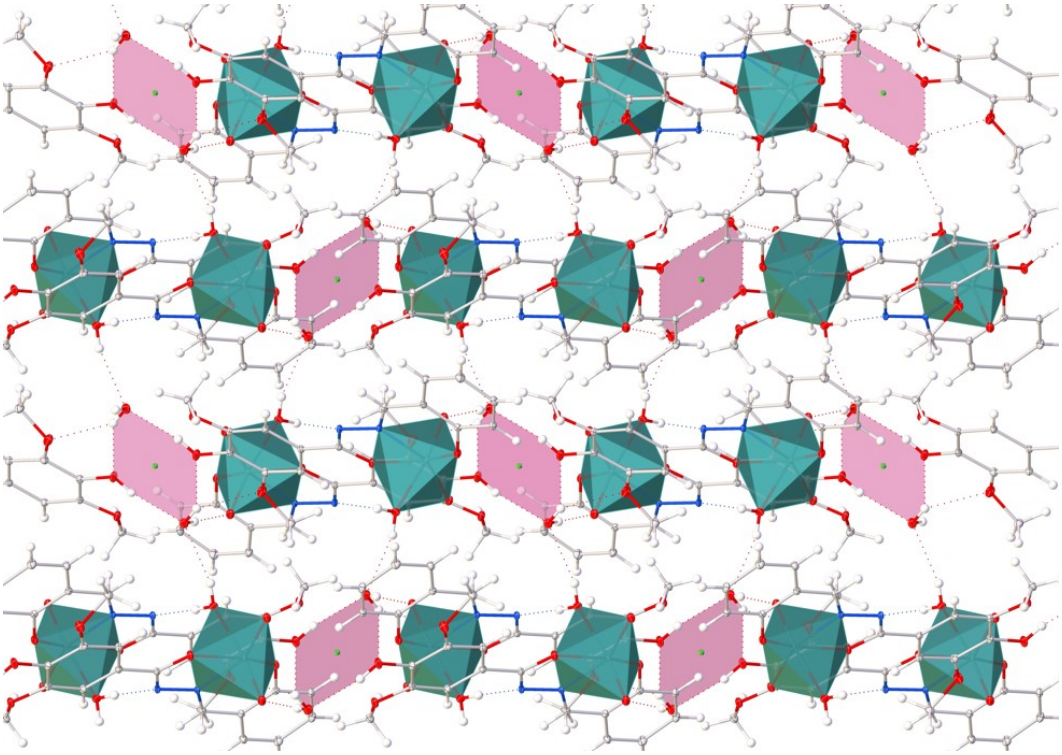

Figure S3. Two-dimensional chains formed through hydrogen bonding are viewed along the crystallographic a-axis. The metal centers are depicted as green polyhedra. The rings formed by hydrogen bonding between lattice water and hydroxyl groups are shown in pink to enhance the visualization of the structure.

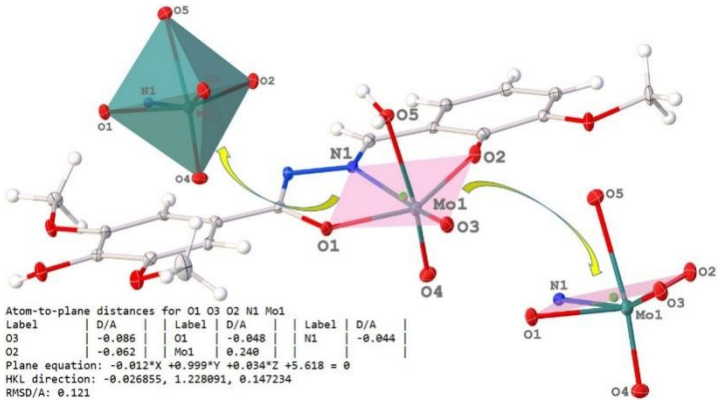

Figure S4. ORTEP diagram of complex **2** depicting octahedral geometry around Mo(VI) center and equatorial plan (the deviation of each atoms and root mean deviation from the plan is shown in the figure).

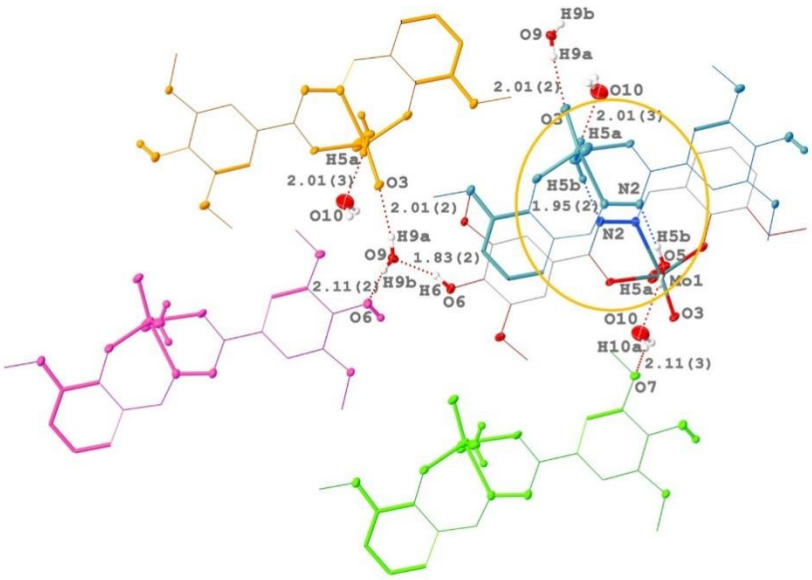

Figure S5. Diagram showing different kind of hydrogen bonding present in complex **2**.

Table S4. Hydrogen Bonds for complex **2.**

D	H	A	d(D-H)/Å	d(H-A)/Å	d(D-A)/Å	D-H-A/°
O5	H5A	O10	0.847(19)	2.01(2)	2.819(5)	160(4)
O5	H5B	N2[1]	0.840(19)	1.95(2)	2.785(4)	177(5)
O6	H6	O9[2]	0.829(19)	1.83(2)	2.626(4)	162(5)
O9	H9A	O3	0.82(2)	2.01(2)	2.807(4)	164(5)
O9	H9B	O6[3]	0.82(2)	2.11(2)	2.924(4)	170(5)
O10	H10A	O7[4]	0.87(2)	2.11(3)	2.930(5)	157(5)

[1]1-x,1-y,1-z; [2]1+x,+y,+z; [3]1-x,1/2+y,3/2-z; [4]1-x,-1/2+y,3/2-z

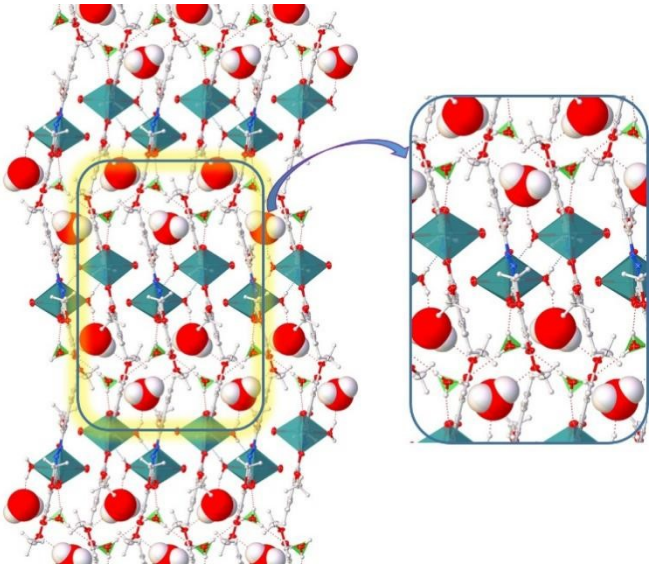

Figure S6. A two-dimensional chain structure is formed through hydrogen bonding, viewed along the crystallographic a-axis. The metal centers are represented as green polyhedra. The

lattice water molecule O10 is depicted using a space-filling model, while water molecule O9 is illustrated as a green triangle to enhance the visualization of the structure.

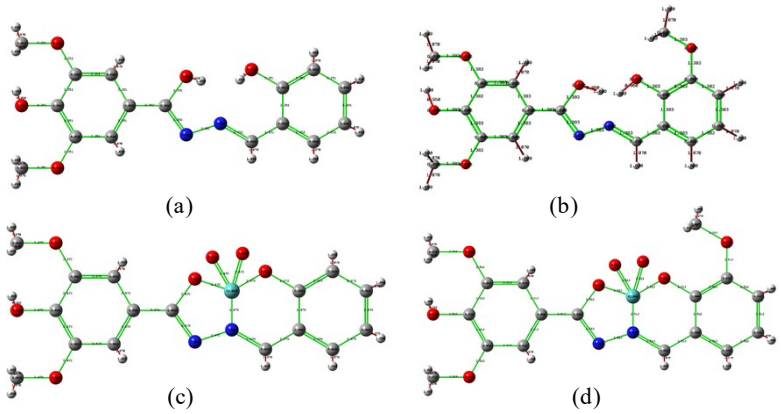

Figure S7. The DFT computations optimized structures for ligands (a) HMB-SA (**I**), (b) HMB-OV (**II**), (c) complex **1** and (d) complex **2**.

Tables S5. FT-IR data for ligands and their complexes.

Compound	**ν (C=O) (Calc.)**	**ν (C=N) (Calc.)**	**ν (N-H) (Calc.)**	**ν_{asymm} (O=Mo=O) (Calc.)**	**ν_{symm} (O=Mo=O) (Calc.)**
HDM-SA(**I**)	1623 (1620)	1585 (1575)	3235 (3240)	-	-
HDM-OV(**II**)	1646 (1644)	1563 (1564)	3232 (3230)	-	-
[MoO_2(HMB-SA).H_2O] (**1**)	-	1565 (1560)	-	943 (942)	910 (908)
[MoO_2(HMB-OV).H_2O] (**2**)	-	1561 (1567)	-	941 (940)	910 (912)
[MoO_2(HMB-SA).H_2O]@rGO (**3**)	-	1558 (1557)	-	940 (939)	908 (907)
[MoO_2(HMB-OV).H_2O]@rGO (**4**)	-	1560 (1562)	-	942 (941)	910 (911)

Tables S6. ^{1}H-NMR spectral values for ligands and complexes.

Compound	**–OH [Calc.]**	**-NH [Calc.]**	**-OCH_3 [Calc.]**	**Other protons [Calc.]**

HDM-SA(**I**)	11.35(1H, s) 9.01(1H, s) [11.38(1H, s) 9.03(1H, s)]	11.87 (1H, s) [11.82 (1H, s)]	3.85 (6H, s) [3.80 (6H, s)]	8.64 (1H, s), 7.53–7.54 (1H, d), 7.31 (1H, t), 7.28–7.30 (1H,d), 6.97–6.99 (4H, m) [8.61 (1H, s), 7.51–7.54 (1H, d), 7.33 (1H, t), 7.26–7.32 (1H,d), 6.96–6.98 (4H, m)]
HDM-OV(**II**)	11.13 (1H, s) 9.26 (1H, s) [11.09(1H, s) 9.24(1H, s)]	11.87 (1H, s) [11.78 (1H, s)]	3.34 (6H, s), 3.80 (3H, s) [3.30 (6H, s), 3.76 (3H, s)]	8.93 (1H, s), 7.70–7.72 (1H, d), 7.49–7.53 (1H, d), 7.24 (1H, s), 7.05–7.09 (1H, s), 6.93–6.95 (1H, t). [8.97 (1H, s), 7.71–7.73 (1H, d), 7.50–7.54 (1H, d), 7.25 (1H, s), 7.07–7.09 (1H, s), 6.95–6.98 (1H, t)]
[MoO_2(HMB-SA).H_2O] (**1**)	8.99(1H, s) [8.92(1H, s)]	-	3.85(6H, s) [3.82(6H, s)]	8.65 (1H, s), 7.27 (1H, d), 7.26(1H, t) 7.15 (1H, t), 7.12–7.13 (1H, d), 7.02–7.04 (1H, s), 6.85–6.92 (1H, s). [8.63 (1H, s), 7.21 (1H, d), 7.22(1H, t) 7.14 (1H, t), 7.12–7.13 (1H, d), 7.03–7.05 (1H, s), 6.87–6.95 (1H, s)]
[MoO_2(HMB-OV).H_2O] (**2**)	9.26(1H, s) [9.22(1H, s)]	-	3.83(6H, s) 3.80 (3H, s) [3.80(6H, s) 3.67(3H, s)]	8.91 (1H, s), 7.29 (1H, d), 7.27 (1H, d), 7.23–7.24 (1H, t), 7.22 (1H, s), 7.00–7.03 (1H, s). [8.78 (1H, s), 7.22 (1H, d), 7.20 (1H, d), 7.23–7.27 (1H, t), 7.19 (1H, s), 7.03–7.05 (1H, s)]

Tables S7. ^{13}C-NMR spectral values for ligands and complexes.

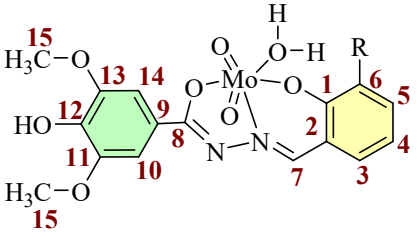

R= H, OCH_3

Compound	C8 [Calc.]	C1 [Calc.]	C7 [Calc.]	Other carbons [Calc.]

HDM-SA(**I**)	162.90 [166.80]	162.53 [161.52]	157.46 [156.82]	147.66, 139.55, 131.35, 129.49, 122.22, 119.45, 118.86, 116.48, 105.55, 56.23 [145.60, 136.53, 131.37, 129.49, 122.22, 117.42, 119.82, 117.49, 104.53, 58.20]
HDM-OV(**II**)	162.51 [160.87]	148.03 [146.50]	147.66 [145.65]	147.52, 147.14, 139.52, 122.27, 119.33, 117.07, 113.73, 105.54, 56.24 [146.50, 147.12, 137.50, 121.27, 118.32, 116.08, 112.70, 103.53, 58.21]
[MoO_2(HMB-SA).H_2O] (**1**)	168.98 [167.85]	159.27 [160.81]	154.84 [153.82]	147.84, 139.74, 134.75, 134.15, 127.70, 120.55, 119.55, 118.57, 105.46, 56.10. [147.84, 137.73, 132.71, 132.15, 125.72, 120.55, 118.55, 119.56, 104.46, 55.10]
[MoO_2(HMB-OV).H_2O] (**2**)	162.52 [164.34]	157.46 [156.45]	147.58 [148.80]	139.54, 133.36, 131.34, 129.48, 122.21, 119.44, 118.85, 116.48, 105.55, 56.22. [135.53, 132.34, 131.35, 128.40, 121.22, 118.47, 119.86, 116.43, 106.50, 57.22]

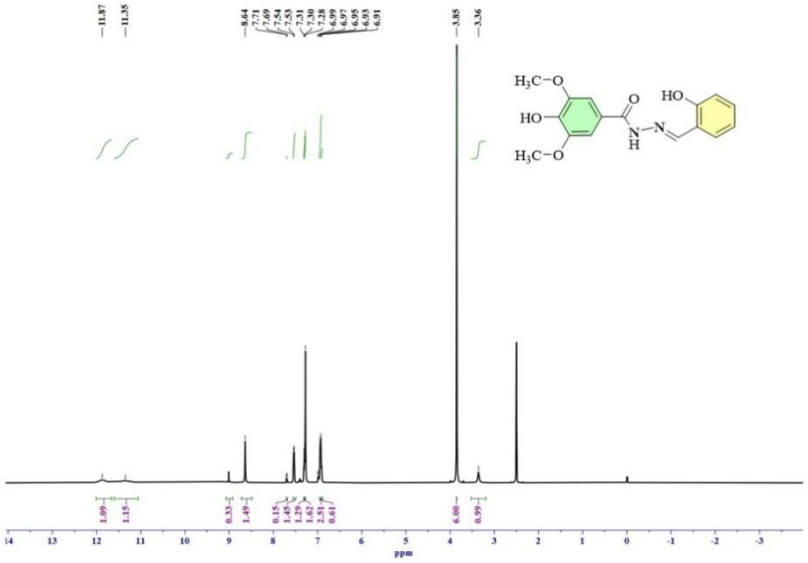

Figure S8. ^{1}H NMR spectra of ligand (**I**) recorded in DMSO-d_6.

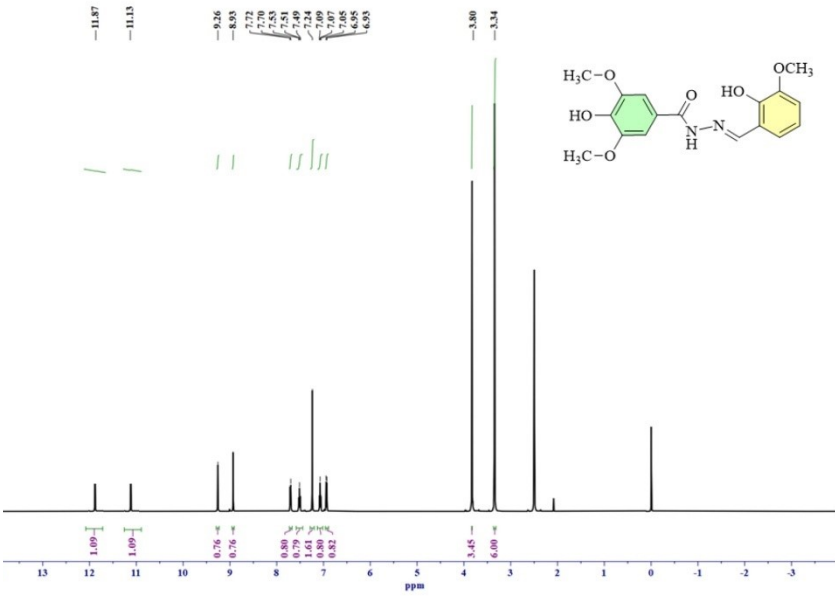

Figure S9. 1H NMR spectra of ligand (**II**) recorded in DMSO-d_6.

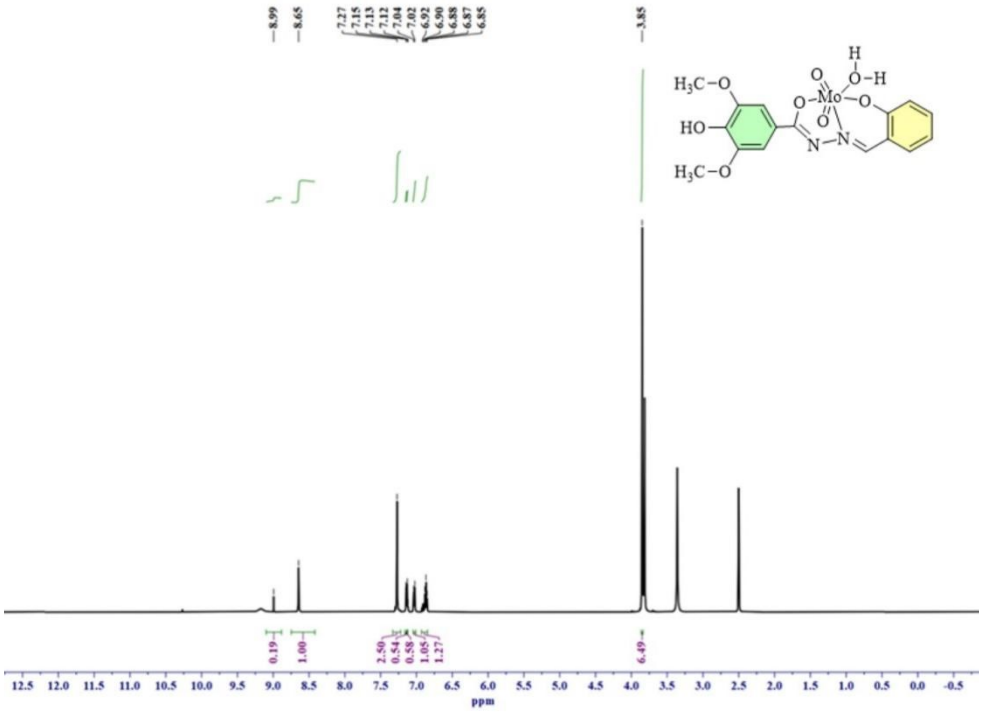

Figure S10. 1H NMR spectra of complex **1** recorded in DMSO-d_6.

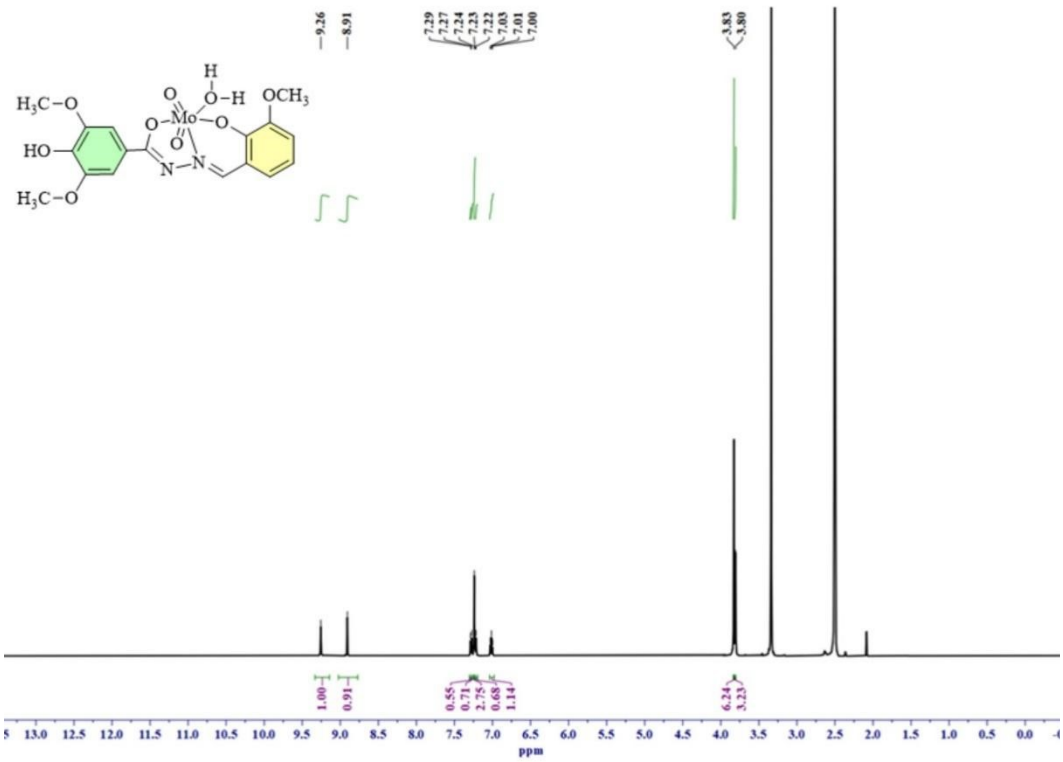

Figure S11. 1H NMR spectra of complex **2** recorded in DMSO-d_6.

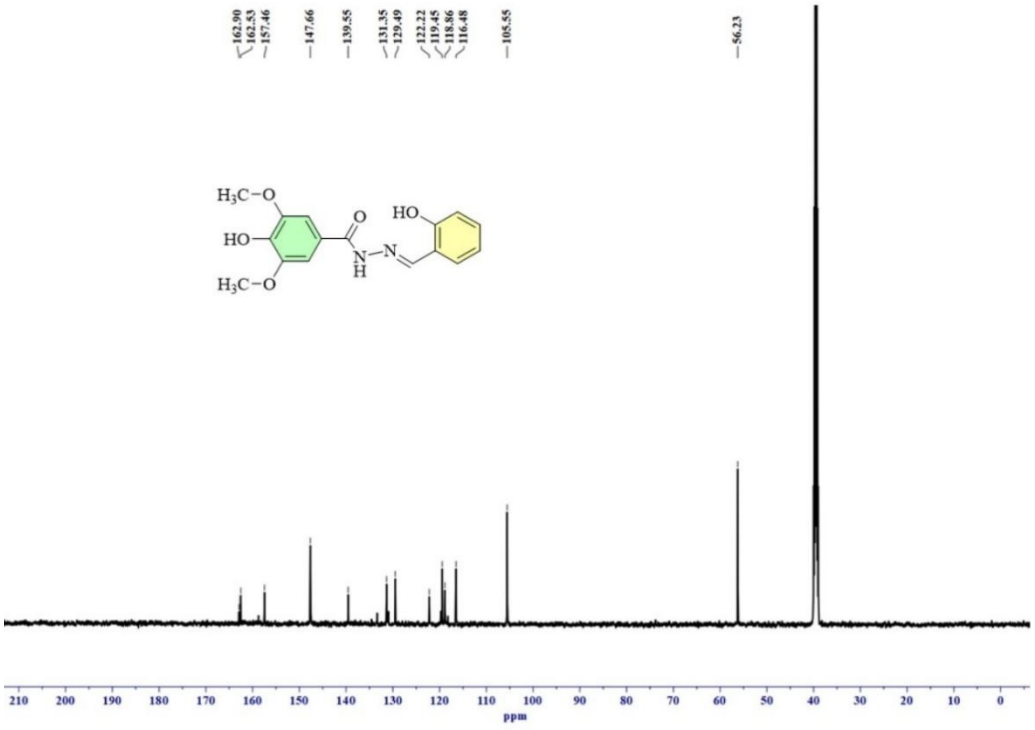

Figure S12. ^{13}C NMR spectra of ligand (**I**) recorded in DMSO-d_6.

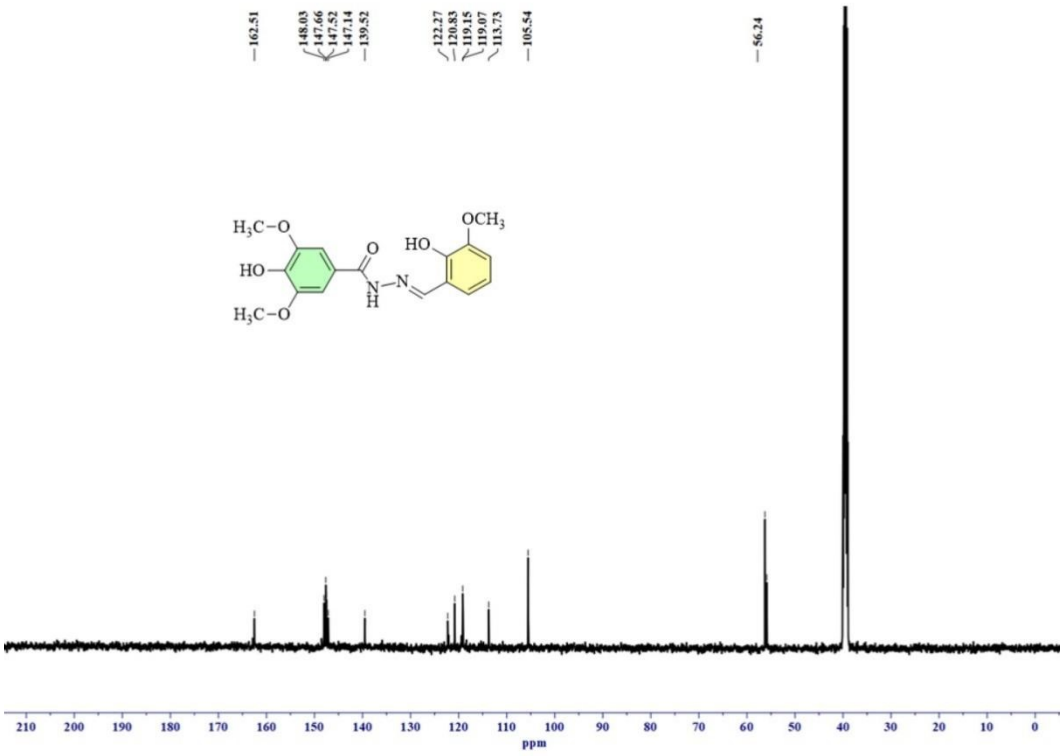

Figure S13. ^{13}C NMR spectra of ligand (**II**) recorded in DMSO-d_6.

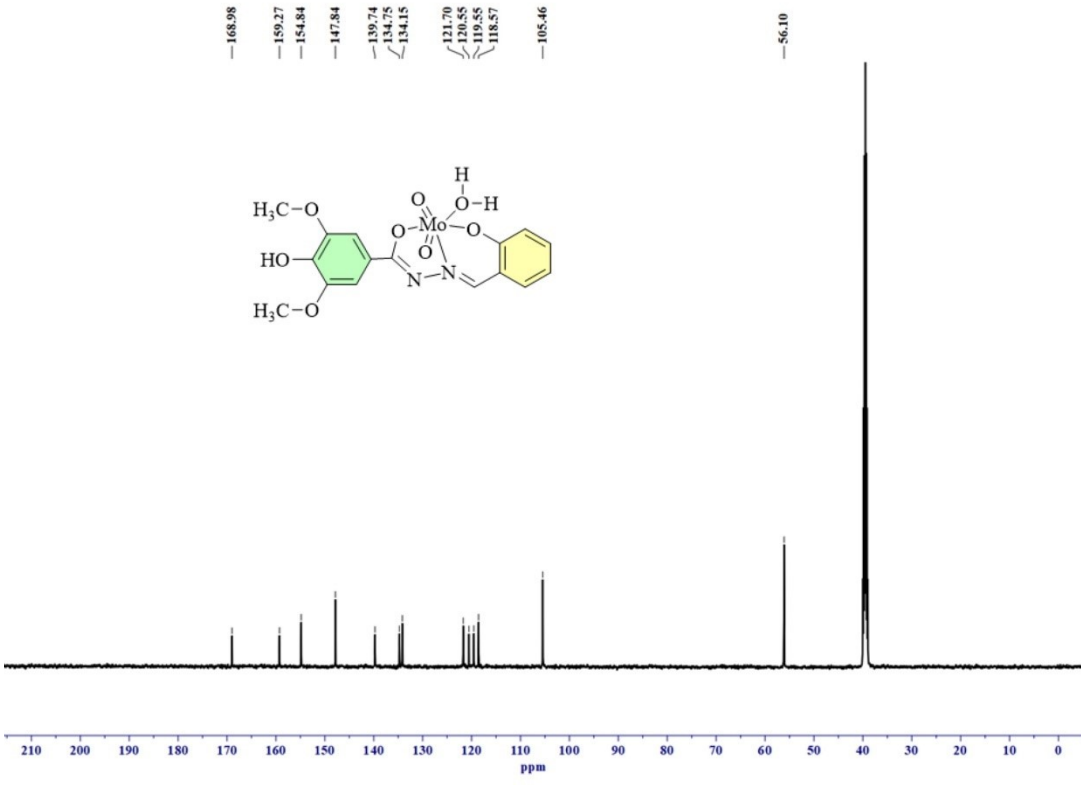

Figure S14. ^{13}C NMR spectra of complex **1** recorded in DMSO-d_6.

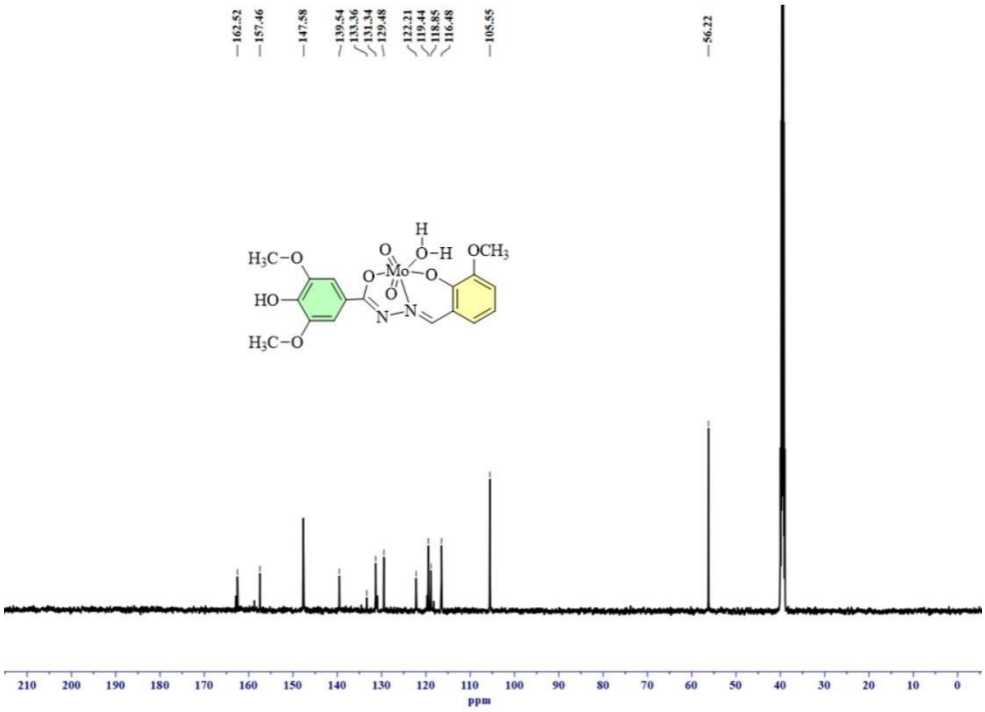

Figure S15. ^{13}C NMR spectra of complex **2** recorded in DMSO-d_6.

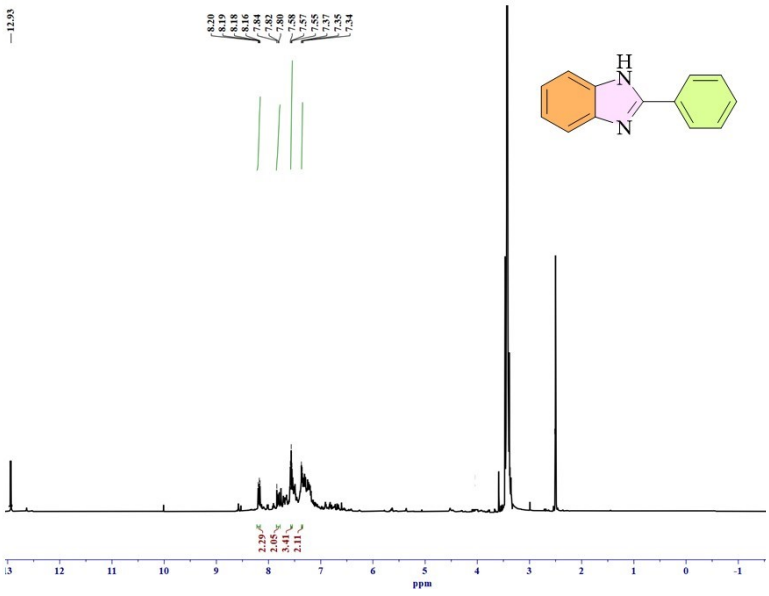

Figure S16. ^{1}H NMR spectra of C_1 compound recorded in DMSO-d_6.

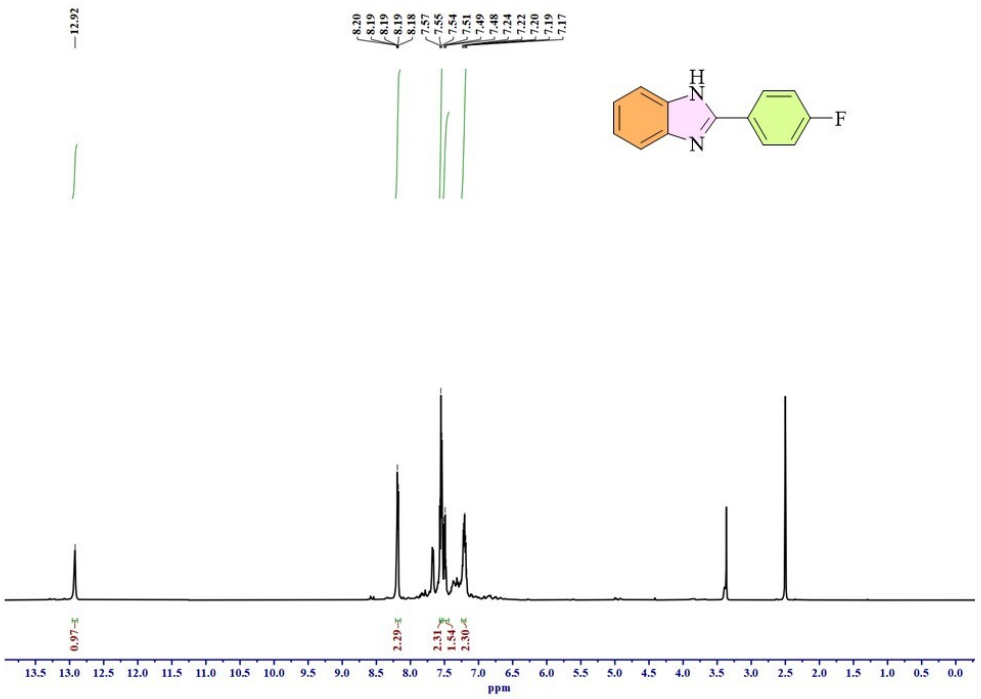

Figure S17. ^{1}H NMR spectra of C_2 compound recorded in DMSO-d_6.

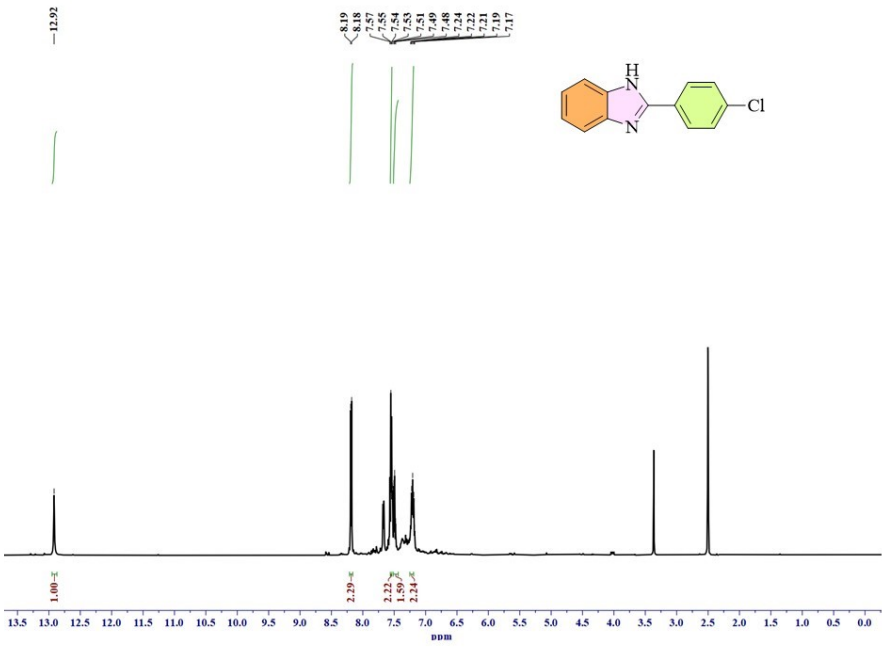

Figure S18. ^{1}H NMR spectra of C_3 compound recorded in DMSO-d_6.

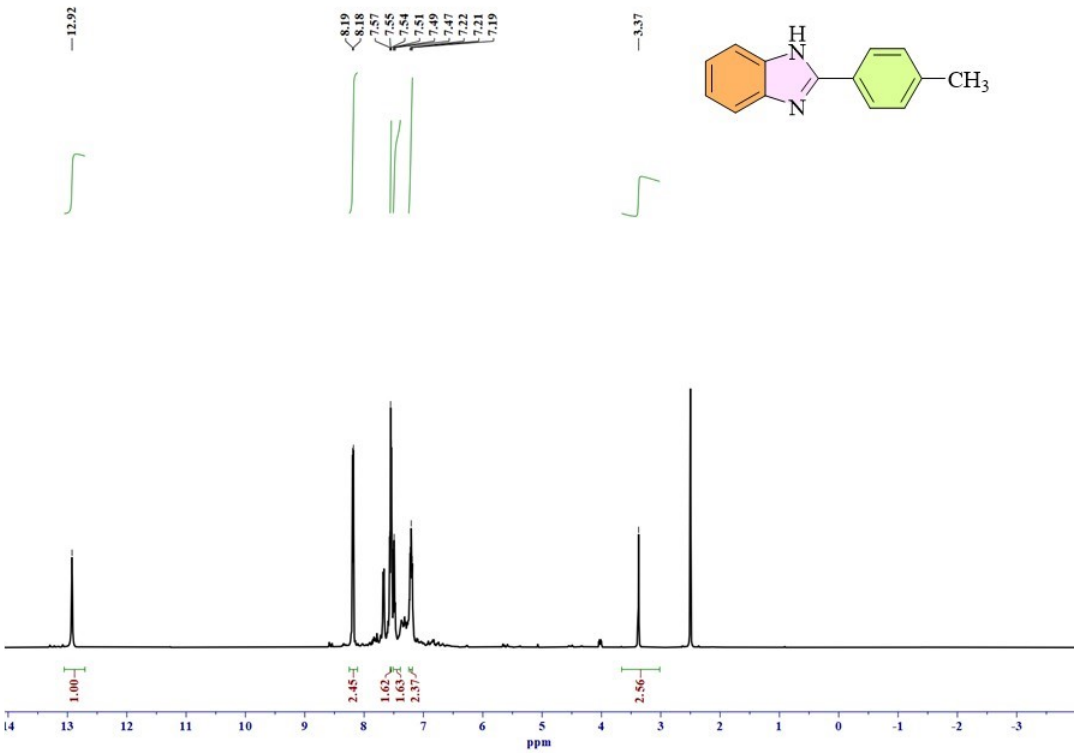

Figure S19. ^{1}H NMR spectra of C_4 compound recorded in DMSO-d_6.

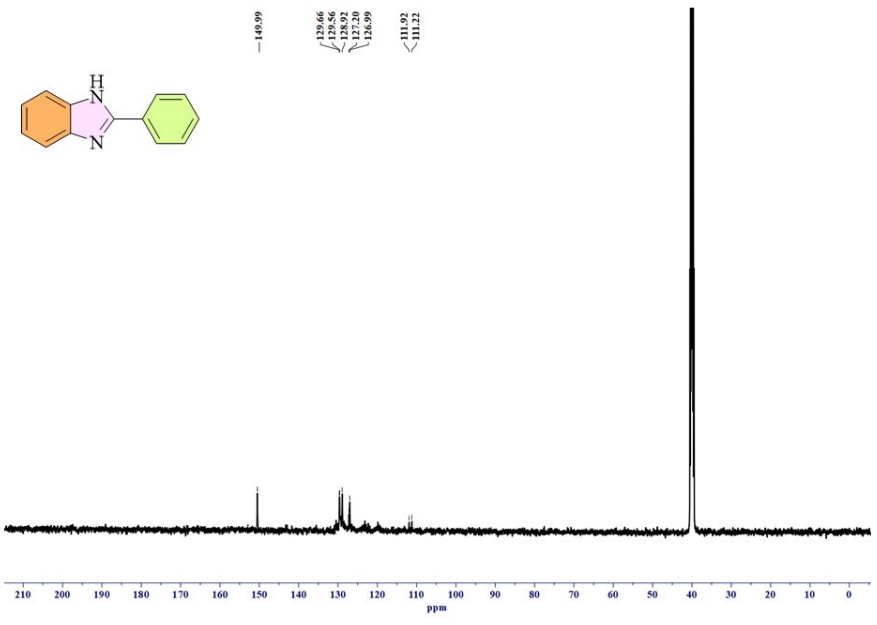

Figure S20. ^{13}C NMR spectra of C_1 compound recorded in DMSO-d_6.

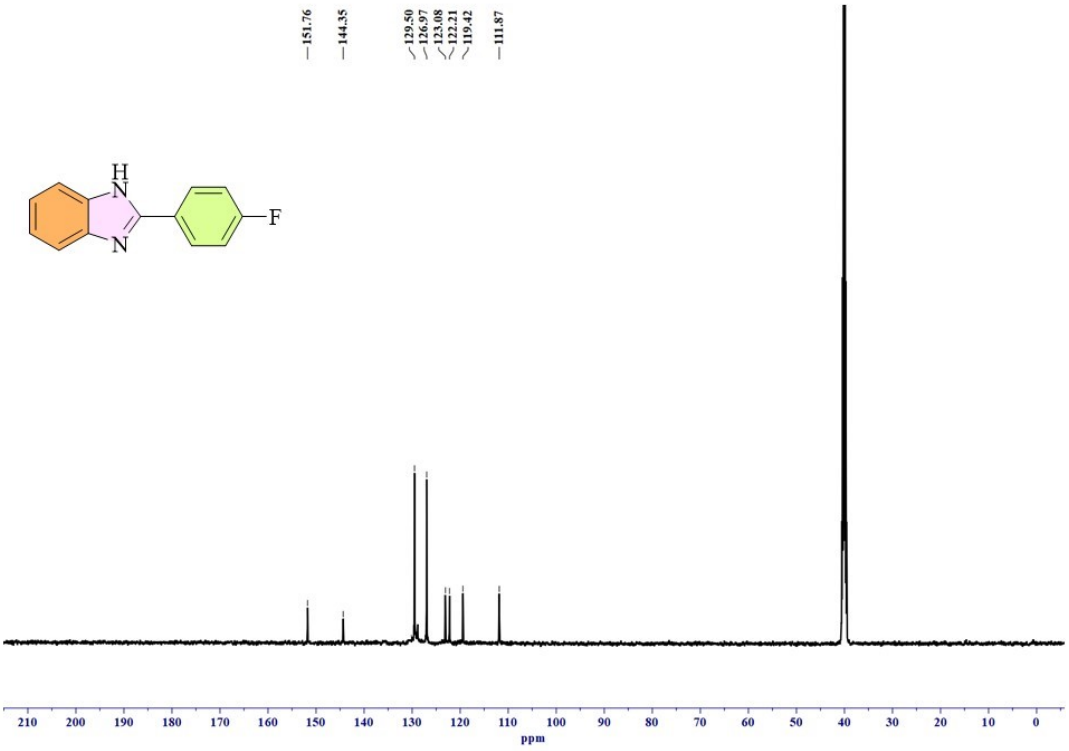

Figure S21. ^{13}C NMR spectra of C_2 compound recorded in DMSO-d_6.

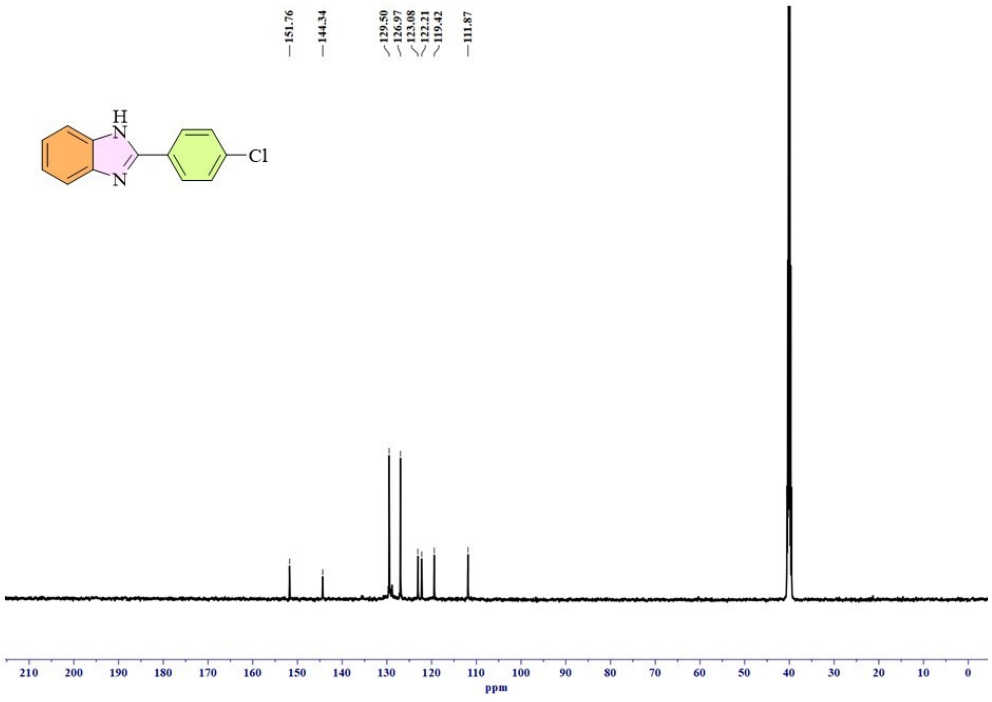

Figure S22. ^{13}C NMR spectra of C_3 compound recorded in DMSO-d_6.

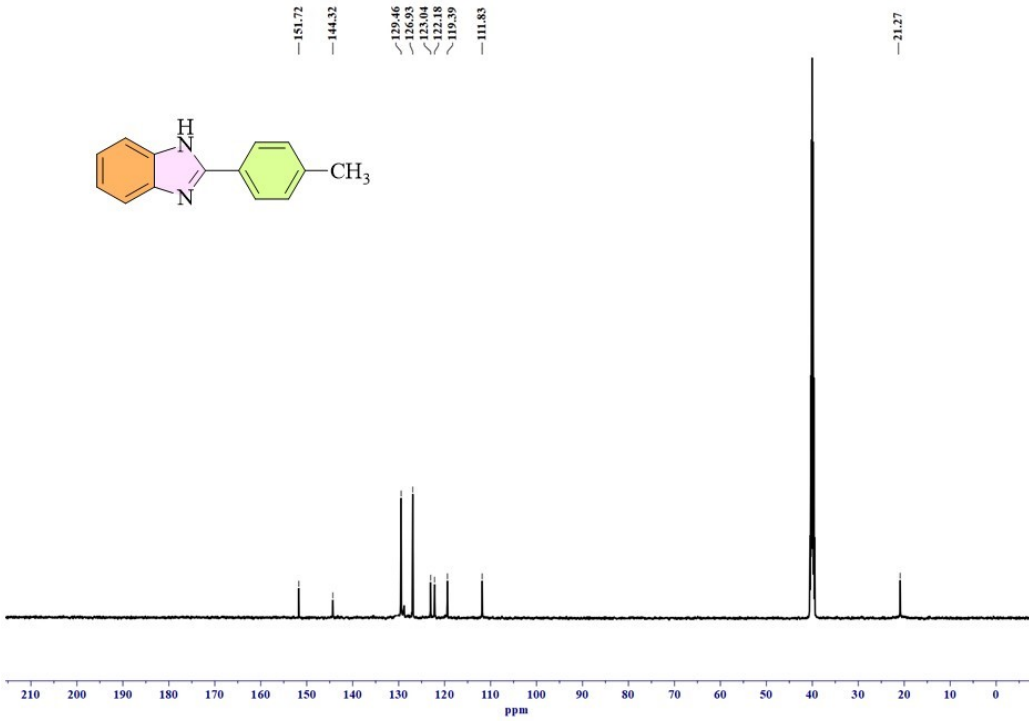

Figure S23. ^{13}C NMR spectra of C_4 compound recorded in DMSO-d_6.

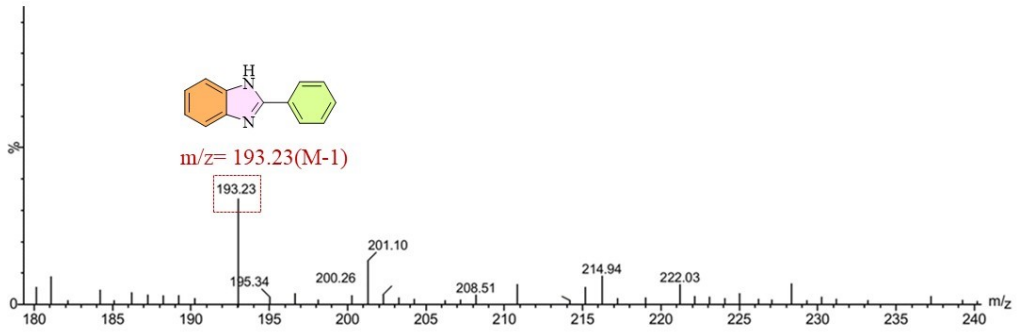

Figure S24. ESI-MS spectra of C_1 compound.

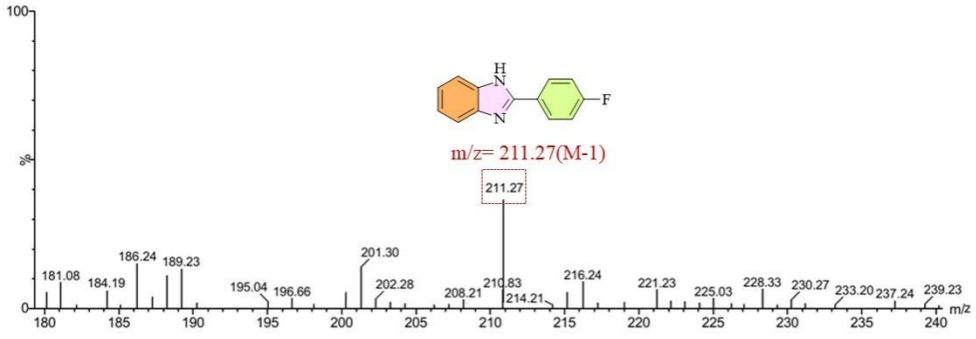

Figure S25. ESI-MS of C_2 compound.

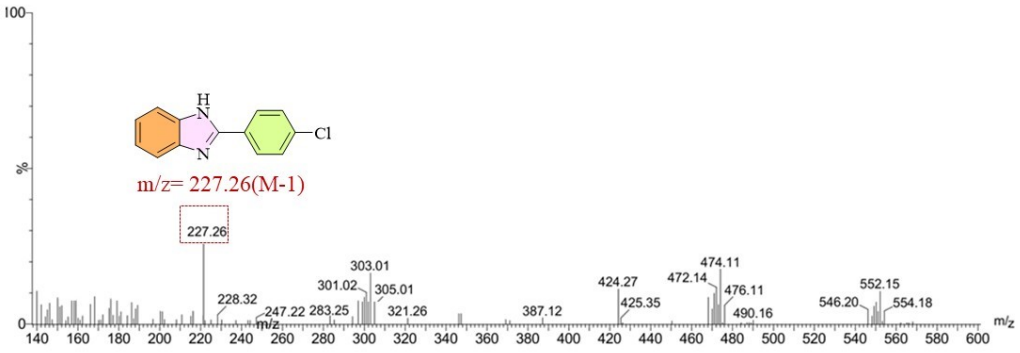

Figure S26. ESI-MS spectra of C_3 compound.

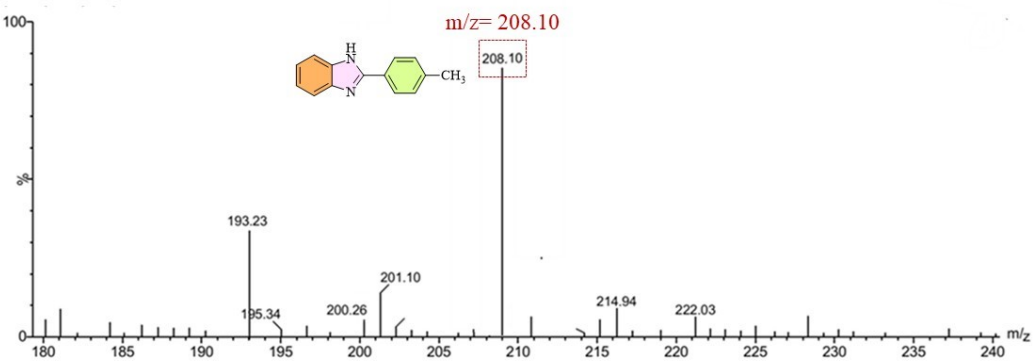

Figure S27. ESI-MS spectra of C_4 compound.

Table S8. The extent of metal leaching after each cycle using catalyst **3** by ICP-OES.

Cycles	Cycle 1	Cycle 2	Cycle 3	Cycle 4
Mo leaching	< 0.2%	< 0.35%	< 0.4%	< 0.5%

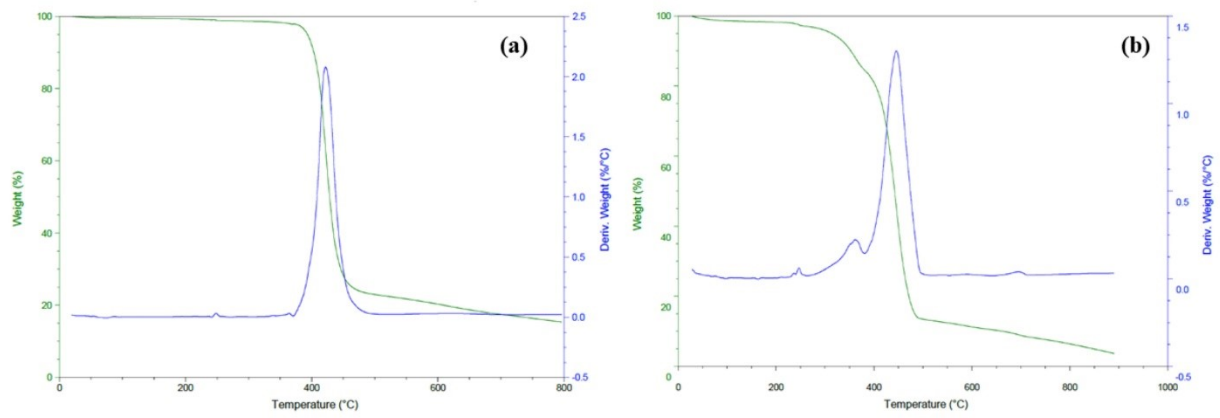

Figure S28. DSC/DTA plots of supported complexes (a) **3** and (b) **4.**

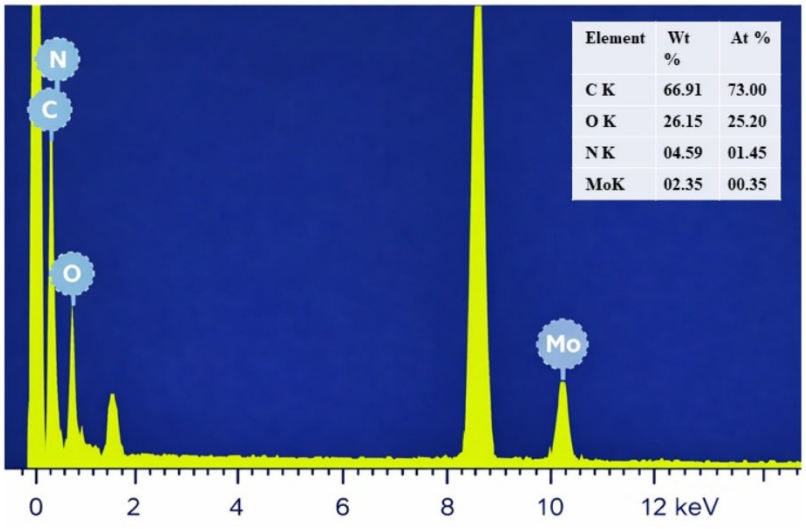

Element	Wt %	At %
C K	66.91	73.00
O K	26.15	25.20
N K	04.59	01.45
MoK	02.35	00.35

Figure S29. HRTEM-EDS image of supported complex **3**.

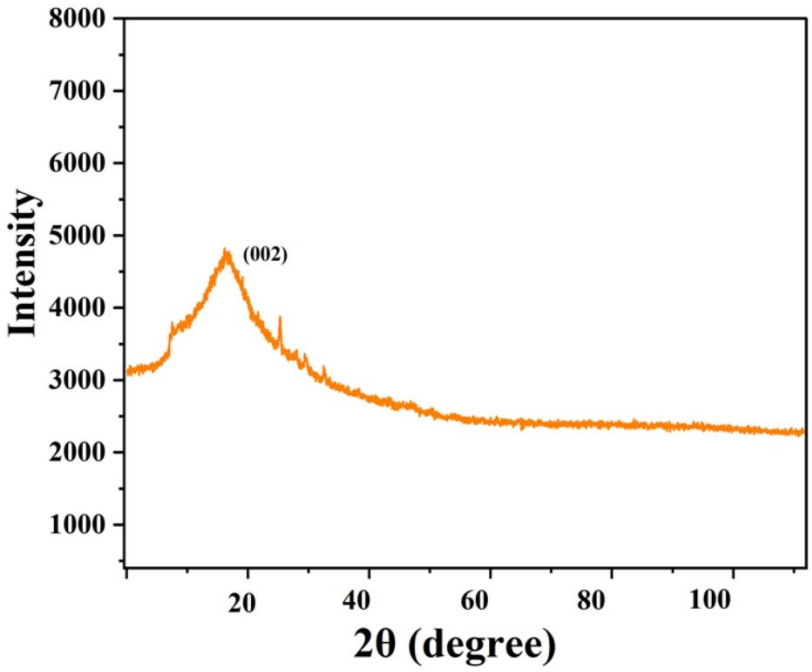

Figure S30. PXRD of catalyst **3** recorded after 1st catalytic run.

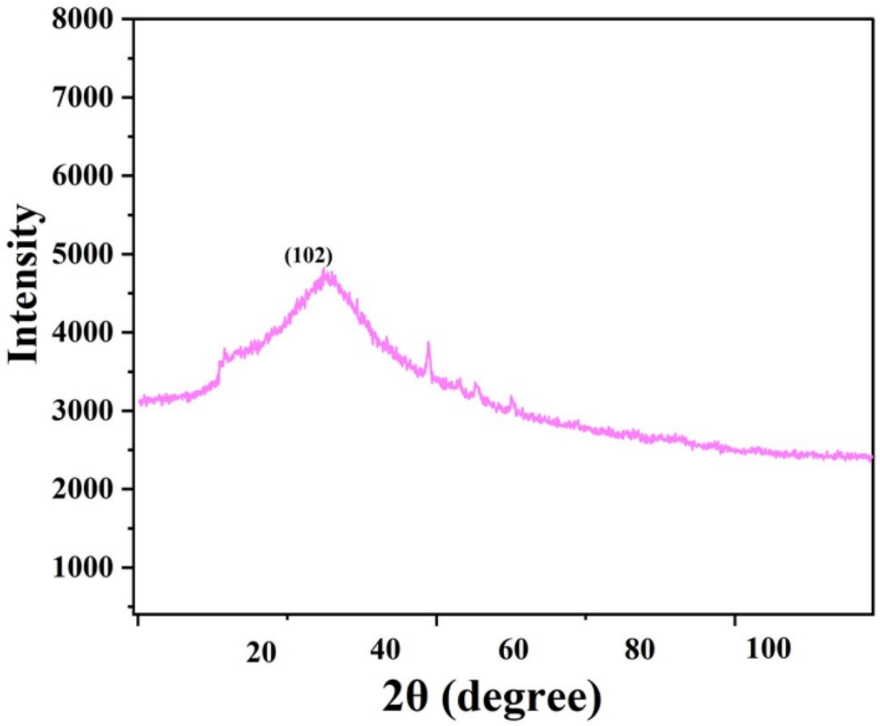

Figure S31. PXRD of catalyst **3** recorded after 2nd catalytic run.

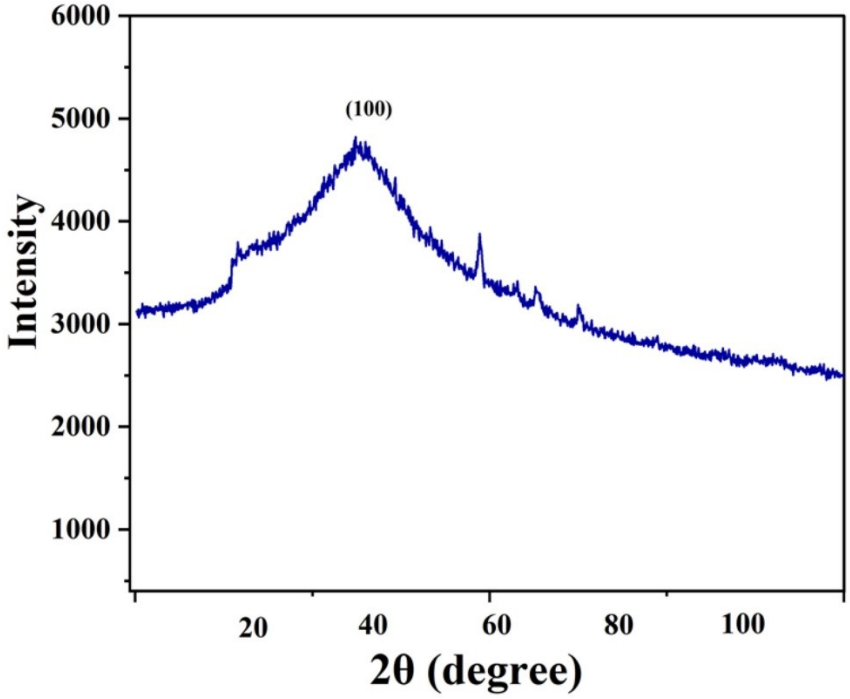

Figure S32. PXRD of catalyst **3** recorded after 3rd catalytic run.

References

1. Bruker, SAINT, version 8.40B, Bruker AXS Inc., Madison, Wisconsin, USA.
2. L. Krause, R. Herbst-Irmer, G. M. Sheldrick and D. Stalke, Comparison of silver and molybdenum microfocus X-ray sources for single-crystal structure determination, *J. Appl. Crystallogr.*, 2015, **48**, 3–10.
3. G. M. Sheldrick, Crystal structure refinement with SHELXL, *Acta Crystallogr., Sect. A*, 2015, **71**, 3–8.
4. G. M. Sheldrick, SHELXT – integrated space-group and crystal-structure determination, *Acta Crystallogr., Sect. C*, 2015, **71**, 3–8.
5. O. V. Dolomanov, L. J. Bourhis, R. J. Gildea, J. A. K. Howard and H. Puschmann, OLEX2: a complete structure solution, refinement and analysis program, *J. Appl. Crystallogr.*, 2009, **42**, 339–341.
6. C. R. Groom, I. J. Bruno, M. P. Lightfoot and S. C. Ward, The Cambridge Structural Database, *Acta Crystallogr., Sect. B*, 2016, **72**, 171–179.
7. M. J. Frisch, G. W. Trucks, H. B. Schlegel, G. E. Scuseria, M. A. Robb, J. R. Cheeseman, G. Scalmani, V. Barone, B. Mennucci, G. A. Petersson, H. Nakatsuji, M. Caricato, X. Li, H. P. Hratchian, A. F. Izmaylov, J. Bloino, G. Zheng, J. L. Sonnenberg, M. Hada, M. Ehara, K. Toyota, R. Fukuda, J. Hasegawa, M. Ishida, T. Nakajima, Y. Honda, O. Kitao, H. Nakai, T. Vreven, J. A. Montgomery Jr., J. E. Peralta, F. Ogliaro, M. Bearpark, J. J. Heyd, E. Brothers, K. N. Kudin, V. N. Staroverov, T. Keith, R. Kobayashi, J. Normand, K. Raghavachari, A. Rendell, J. C. Burant, S. S. Iyengar, J. Tomasi, M. Cossi, N. Rega, J. M. Millam, M. Klene, J. E. Knox, J. B. Cross, V. Bakken, C. Adamo, J. Jaramillo, R. Gomperts, R. E. Stratmann, O. Yazyev, A. J. Austin, R. Cammi, C. Pomelli, J. W. Ochterski, R. L. Martin, K. Morokuma, V. G. Zakrzewski, G. A. Voth, P. Salvador, J. J. Dannenberg, S. Dapprich, A. D. Daniels, O. Farkas, J. B. Foresman, J. V. Ortiz, J. Cioslowski and D. J. Fox, *Gaussian 09*, Revision D.01, Gaussian, Inc., Wallingford, CT, 2013.
8. A. D. Becke, Density-functional thermochemistry. III. The role of exact exchange, *J. Chem. Phys.*, 1993, **98**, 5648–5652.
9. J. Gauss, Effects of electron correlation in the calculation of nuclear magnetic resonance chemical shifts, *J. Chem. Phys.*, 1993, **99**, 3629–3643.

10. J. R. Cheeseman, G. W. Trucks, T. A. Keith and M. J. Frisch, A comparison of models for calculating nuclear magnetic resonance shielding tensors, *J. Chem. Phys.*, 1996, **104**, 5497–5509.
11. K. Wolinski, J. F. Hinton and P. Pulay, Efficient implementation of the gauge-independent atomic orbital method for NMR chemical shift calculations, *J. Am. Chem. Soc.*, 1990, **112**, 8251–8260.